2011

Synthesis, co-polymerisation and electrochemical evaluation of novel ferrocene-pyrrole derivatives

Mary Deasy
Technological University Dublin, mary.deasy@tudublin.ie

Eithne Dempsey
Maynooth University

Geok Hong Soon
Technological University Dublin, Tallaght, Dublin, geok.hongsoom@tudublin.ie

See next page for additional authors

Recommended Citation

Hong Soon, G., Deasy, M. & Worsfold, O. (2011). Synthesis, co-polymerisation and electrochemical evaluation of novel ferrocene-pyrrole derivatives. *Analytical Letters*, vol. 44, no. 11. doi:10.1080/00032719.2010.539729

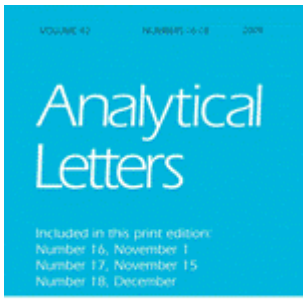

Synthesis, co-polymerisation and electrochemical evaluation of novel ferrocene-pyrrole derivatives.

Journal:	*Analytical Letters*
Manuscript ID:	LANL-2010-0295
Manuscript Type:	Special Issue: KAC-10
Date Submitted by the Author:	12-Mar-2010
Complete List of Authors:	Soon, Geok; Institite of Technology Tallaght Deasy, Mary; Institute of Technology Tallaght Worsfold, Oliver; Newcastle University Dempsey, Eithne; Institute of Technology Tallaght
Keywords:	ferrocene pyrrole derivatives , thin film deposition, co-polymerisation

Synthesis, co-polymerisation and electrochemical evaluation of novel ferrocene-pyrrole derivatives.

Geok Hong Soon[1], *Mary Deasy*[1], *Oliver Worsfold*[2] *and Eithne Dempsey**[1]

[1]Centre for Research in Electroanalytical Technologies (CREATE), Institute of Technology Tallaght, Tallaght, Dublin 24, Ireland.

[2]Business Development Directorate, Stephenson Building, Newcastle University, Newcastle Upon Tyne, NE1 7RU, U.K.

Abstract

New ferrocene derivatives, (6-(4-(1H-pyrrol-1-yl)phenoxy)hexyl) ferrocene (**1**) and ((4-(1H-pyrrol-1-yl)phenoxy)carbonyl) ferrocene (**2**)were synthesised, characterised and electrochemically evaluated as redox active films formed via anodic oxidation with pyrrole. Thin film studies were conducted and films formed from both compounds resulted in a stable Fe $^{II/III}$ redox couple with E^o = 0.035V and 0.365V vs. Ag/Ag^+ for **(1)** and **(2)** respectively. Both potential sweeping and chronocoulometry were employed for film formation with the former resulting in controllable, reproducible film deposition. Growth conditions and solution concentrations were varied in order to assess influence on electrochemical behavior. Surface coverage's were of the order 10^{-8}-10^{-9} mol cm^{-2}, surface confined behavior (i_p vs. ν) was evident up to 0.2 V s^{-1} with semi-infinite diffusion (i_p vs. $\nu^{1/2}$) dominating at higher scan rates. Laviron theory was employed where possible for the determination of electron transfer co-efficient and rate constants.

*Corresponding author Eithne.dempsey@ittdublin.ie

tel +353 1 4042862 fax +353 1 4042404

geok.hong@itnet.ie; mary.deasy@ittdublin.ie; oliver.worsfold@ncl.ac.uk

Key words : ferrocene pyrrole derivatives, co-polymerisation, thin film deposition

Introduction

Organometallic compounds, particularly metallocenes, have established a significant role in a range of sensor applications over recent decades (Forrow 2005). Unlike other organometallic compounds, the properties of metallocenes, in terms of electrochemistry in particular, can readily be modified by substitution on one or both cyclopentadienyl rings. A recent review describes polymers with conjugated matrices which incorporate metallocene complexes with two cyclopentadienyl ligands and their derivatives (Vorotynstev 2008).

A wide variety of heterocycles bearing tethered ferrocene groups have been prepared and electropolymerised to form conducting electroactive polymers, with a range of applications (Chen 2002). Pyrroles are excellent monomers for the electropolymerisation of polymer films containing redox active centers, and the synthesis and applications of polypyrrole films containing metal complexes have been reviewed (Deronzier 1996). The binding of electrocatalytically active redox species within conducting polymer films opens up possibilities for the design of electron transfer pathways between immobilised enzymes and electrode surfaces (Schuhmann 1997). Other reports of redox active co-polymer films include long and short chain osmium and ruthenium bipyridine modified pyrrole derivatives (Warren 2008, Habermuller 2000, Reiter 2001, Schuhmann 1993, Ochmanska 1989).

Ferrocene and their derivatives have made frequent appearances in reviews and reports on biosensors as redox mediators (electron shuttles) for rapid electron transfer between

active sites of enzymes and electrodes (Vorotyntsev 2008, Hudson 2001, Rahman 2008). Due to a combination of catalytic efficiency, stability in the reduced form, pH independent redox potentials, ease of synthesis and versatility of substitution, ferrocene exceeds other organometallic compounds with respect to biosensor applications. Moreover, ferrocenes are small in size and sufficiently mobile to penetrate the enzyme active site (Forrow 2002). However, with its chemical structure of two π-bonding cyclopentadienyl rings, ferrocene itself is naturally hydrophobic, limiting its use in aqueous media. Intensive efforts have been made to modify one or both of the π-bonding cyclopentadienyl rings in order to render ferrocene more hydrophilic or otherwise more suitable as a redox mediator (Laselle 1994 and Cass 1984).

It is well known that the nature of substituents affects the redox potentials of ferrocenes, i.e. electron withdrawing groups, such as carboxylic acids or carbonyl groups, shift $E_{1/2}$ in the anodic direction, while electron donating substituents, such as methyl- or amino, shift $E_{1/2}$ in the cathodic direction (Tustin 2007 and Forrow 2002). The charge on ferrocene also plays an important role in its ability to act as a mediator. No direct correlation between the mediation rate constant (k_{med}) and the redox potential of the ferrocene derivatives has been observed (Bartlett 1991 and Ryabov 2001). Hence, ferrocene derivatives of low redox potentials do not necessarily possess high k_{med} values. Conversely, biosensor systems of high redox potential are susceptible to interference in real samples and, more importantly, can be fouled at a high substrate concentration (Ruan 2001).

Forrow et al 2002, reported synthesis and characterisation of a series of ferrocenylaminoalcohols in a search for suitable redox mediators for glucose biosensors. In their report, the electrochemical and kinetic data of the ferrocene derivatives were tabulated to study the influence of the substituents in ferrocene on redox potentials and mediation rate constant. It was agreed that the electronic effects of the substituents influence the redox potentials of the ferrocene derivatives but the effects diminish if the substituents were too far (n > 3 or 4) from the ferrocene molecule. The degree of solubility in aqueous medium is dependent on the nature of substituents, e.g. NH_2 > OH > $CONH_2$.

An electrochemical enzyme (glucose oxidase) electrode based on a ferrocene-containing redox polymer (ferrocene-containing cross-linked polyallylamine) was cross-linked using glutaraldehyde and bovine serum albumin (BSA) on a glassy carbon electrode surface. The electrochemical behavior of the redox polymer was found to be almost completely based on a semi-infinite diffusion process (Koide 1991). Brown et al developed electropolymerised films of tetraaminophthalocyanine (TAPc) with ferrocene (Fc), which produced a three-dimensional network of Fc active sites used for the detection of glucose. Following polymerisation, glucose oxidase was immobilised onto the TAPc/Fc films and the biosensor was then employed in the detection of glucose (detection limit 5 μM). Under stirred conditions, the biosensor reached a limiting current in approximately 10–15 s (Brown 2005). Naruhide et al 2008 reported the application of electrodeposited single-wall carbon nanotubes (SWCNT) as an immobilisation matrix for the construction of an amperometric glucose biosensor. The SWCNT attached electrode surface was

subsequently modified with glucose oxidase (GOD) and 11-(ferrocenyl)-undecyltrimethylammonium bromide (FTMA). The formation of the biosensor was controlled by constant potential electrolysis. The cyclic voltammetric results implied that direct electron transfer occurred between the active centre of immobilised GOD and the modified surface of the electrode. The electron-transfer coefficient was 0.70±0.3 and electron-transfer rate constant was evaluated to be 2.69±0.03 s^{-1}. The electrode retained 78.62% of its initial response after 50 cycles.

Having taking into account recent literature and the trends observed with various electron donating/withdrawing substituents (Forrow 2002) incorporated into ferrocene, several candidate structures were selected for synthesis and characterisation. These include (6-(4-(1H-pyrrol-1-yl) phenoxy) hexyl) ferrocene **(1)** and ((4-(1H-pyrrol-1-yl) phenoxy) carbonyl) ferrocene (**2**) which will be the subject of this study. The attached pyrrole monomer unit facilitated polymer growth via co-polymerisation with pyrrole to form redox active polymer films. This investigation forms the first step in the evaluation of these immobilised redox species as potential candidates for effective oxidase enzyme (glucose/glutamate) mediation.

Experimental

Materials and Methods

All solvents employed were HPLC grade, obtained from either Sigma- Aldrich or Lennox Laboratory Supplies. All ferrocene starting materials were obtained from Sigma- Aldrich. All deuterated solvents employed in NMR studies were obtained from Sigma-Aldrich and

contained 0.03% TMS as internal standard. All isolated products were dried under vacuum before characterisation and further use. Pyrrole (≥ 99%) was supplied by Fisher Scientific and was purified with aluminium oxide before use.

Instrumentation

Melting point analyses were carried out using a Stewart Scientific SMP1 melting point apparatus and were uncorrected. Elemental analyses were carried out at University College Dublin, Dublin, Ireland. Infrared spectra were obtained from a Nicolet *Impact* 410 FT-IR spectrometer using the Omnic software. Solid samples were prepared as dispersion in KBr disks. ^{1}H and ^{13}C NMR spectroscopy were carried out on a Joel JNM-LA 300 FT-NMR 300 MHz spectrometer using $CDCl_3$ as the solvent unless stated, and tetramethylsiliane (TMS) as the internal standard. Chemical shifts were expressed in parts per million (δ) downfield from the internal standard. Cyclic voltammetry and amperometry experiments were carried out using CH instruments CHI 660, CHI 750, CHI 420 and CHI 900 potentiostats. A single-compartment electrochemical cell was used with a glassy carbon working electrode, a platinum counter electrode and Ag/ AgCl | KCl (3 M) reference for aqueous solutions. For the non-aqueous solutions, the reference electrode used was a silver wire in contact with a solution of acetonitrile and $AgNO_3$ (10 mM) and 0.1 M of the same supporting electrolyte as employed in the cell and was referred as Ag | Ag^+.

***Synthesis of (6-(4-(1H-pyrrol-1-yl) phenoxy) hexyl) ferrocene* (1)**

Anhydrous potassium carbonate (1.38 g, 10 mmol) and 4-(1H-pyrrol-1-yl) phenol (0.64 g, 4 mmol) were added to a stirred solution of acetonitrile containing bromohexylferrocene (1 g, 3 mmol). The reaction mixture was then refluxed under nitrogen for 36 h. The reaction mixture was cooled to room temperature and filtered under reduced pressure. The filtrate was dissolved in 6 mL dichloromethane and finally triturated in 10 mL methanol to produce a bright yellow solid. The product mixture was filtered and the yield was 1.13 g (92%).

TLC (eluent: hexane: ethyl acetate, 90 : 10) revealed a spot with R_f of 0.51. m. p. 148 - 151 ^{o}C. Found C, 72.93; H, 6.78; N, 3.27; Fe, 13.95, requires C, 73.07; H, 6.84; N, 3.28; Fe, 13.07. υ_{max}/ cm^{-1} 2937 (N-H) 2454 (C-H) 1525 (C-O). δ_H (300 MHz, $CDCl_3$) 4.26 (5H, m, H_c x 5), 4.52 (2H, d, H_b x 2), 4.98 (2H, d, H_a x 2), 6.35 (2H, d, H_k x 2), 7.07 (2H, d, H_j x 2), 7.04 (2H, d, H_g x 2) and 7.33 (2H, d, H_h x 2). δ_c 111.1 (C_k x 2), 121.9 (C_g x 2), 122.3 (C_h x 2), 123.9 (C_j x 2), 137.1 (C_c x 5), 137.4 (C_b x 2), 137.8 (C_i), 141.2 (C_a x 2), 148.3 (C_f), 150.4 (C_d), 168.1 (C_e).

***Synthesis of ([4-(1H-pyrrol-1-yl) phenoxy] carbonyl) ferrocene* (2)**

A mixture of ferrocenecarboxylic acid (0.46 g, 2.02 mmol), *N*, *N*′-dicyclohexylcarbodiimide (DCC) (0.60 g, 2.91 mmol), 4-(dimethylamino) pyridine (0.24 g, 1.97 mmol) and 4-(1H-pyrrol-1-yl) phenol (0.32 g, 1.98 mmol) were refluxed in 40 mL anhydrous dichloromethane. The reaction was carried out under nitrogen for 48 h. Subsequent to cooling the reaction mixture, 50 mL dichloromethane was added. The

mixture was filtered through a bed of silica. An additional 50 mL dichloromethane was used to recover any desired product left in the silica bed. The solvent was then removed under vacuum. To prompt recrystallisation, the residue was dissolved in a minimum amount (~ 2 mL) of dichloromethane was added into methanol (~ 10 mL). The resulting yellow powder was washed with hot hexane to get rid of traces of DCC. Following filtration, the residue was recrystallised twice in a mixture of dichloromethane: methanol (2 mL : 18 mL). The product was filtered and dried. The yield was 0.36 g (49%).

TLC (eluent: hexane: ethyl acetate, 70 : 30) revealed a spot with R_f of 0.51. m. p. analysis was recorded as 135 - 139 ^{o}C. Found C, 67.51; H, 5.10; N, 3.44; Fe, 15.00, requires C, C, 67.95; H, 4.62; N, 3.77; Fe, 15.04. υ_{max}/ cm^{-1} 1743 (C=O), 1525 (C-N). δ_H (300 MHz, $CDCl_3$) 1.40 (4H, m, H_{f+q}), 1.46 (2H, m, H_e), 1.56 (2H, m, H_h), 2.32 (2H, t, H_d), 3.97 (2H, t, H_i), 4.13 (5H, m, H_c x 5), 3.95 & 4.00 (4H, d, H_a x 2 + H_b x 2), 6.32 (2H, m, H_m x 2), 6.95 (H, d, H_j x 2), 7.00 (2H, d, H_l x 2), 7.31 (2H, d, H_k x 2). δ_c 25.9 (C_g), 29.6 (C_f), 30.1 (C_h), 30.8 (C_d), 31.3 (C_e), 69.9 (C_i) 111.2 (C_m x 2), 116.1 (C_j x 2), 123.0 (C_k x 2), 125.7 (C_l), 133.3 (C_o), 135.8 (C_q), 136.1 (C_a x 2), 137.1 (C_c x 5), 140.6 (C_b x 2) 154.7 (C_p).

Procedures

Co-polymerisation of ferrocene derivatives and pyrrole using cyclic voltammetry

Prior to each experiment, glassy carbon electrodes (geometric area, 0.0707 cm^2) were polished with 1.0, 0.3, 0.05 μm alumina powder to create a mirror finish, the electrode was sonicated in deionised water and finally washed and dried using Argon at room

temperature. 3 mL of ferrocene derivative, ((4-(1H-pyrrol-1-yl)phenoxy)carbonyl) ferrocene (**2**) or (6-(4-(1H-pyrrol-1-yl)phenoxy)hexyl) ferrocene (**1**) (1 – 5 mM) and pyrrole (0.1 to 5 mM) in acetonitrile/0.1 M $TBAPF_6$ was cycled at 100 mV s^{-1} for (1-5 cycles) on the surface of glassy carbon working electrode from -0.4 V to 1 V vs. Ag | Ag^+. Following polymer growth, the electrode was rinsed with acetonitrile to remove unpolymerised material. The polymer films was then stabilised in a fresh solution of acetonitrile/0.1 M $TBAPF_6$ over the range 0.2V to 0.7V for ferrocene derivative (**1**), -0.2V to 0.4V for ferrocene derivative (**2**) for 25 cycles at 25 mV s^{-1}. A scan rate study (1 – 1000 mV s^{-1}) was performed for each film over the range 0.2V to 0.7V for ferrocene derivative (**2**), -0.2V to 0.4V for ferrocene derivative (**1**). The films were also examined in a number of aqueous buffers 0.1 M PBS pH 7.4, 0.1 M KCl in PBS pH 7.4 (0.1 M), 0.1 M Tris buffer pH 7.4, 0.1 M NH_4PF_6 and 0.1 M $LiClO_4$.

Co-polymerisation of ferrocene derivatives and pyrrole using chronocoulometry

A solution of 3 mL of ferrocene derivative, ((4-(1H-pyrrol-1-yl)phenoxy)carbonyl) ferrocene (**2**) and (6-(4-(1H-pyrrol-1-yl)phenoxy)hexyl) ferrocene (**1**) (1 mM) and pyrrole (0.5 mM) in acetonitrile/0.1 M $TBAPF_6$ was employed with the following parameters: Potential: 0 (initial) and 0.65 V (final) with 1 step and pulse width of 1000 sec, sample interval of 0.063 sec. Following polymer growth, the co-polymer films were stabilised using the same conditions as before.

Research and Discussion

Two new pyrrole-ferrocene derivatives with differing spacer linkages were prepared according to the synthetic routes described in Schemes 1 and 2. The ferrocene compounds used as starting materials were known compounds and commercially available. The originality of the synthetic routes reported here lies in the respective coupling reactions with 4-(1H-pyrrol-1-yl) phenol and their respective reaction conditions.

The shorter chain ([4-(1H-pyrrol-1-yl) phenoxy] carbonyl) ferrocene **(2)** was prepared using a modified Steglich esterification procedure using DCC and DMAP as condensing agent and catalyst respectively. The yellow solid product was isolated in moderate yield (49%), following recrystallisation and exhaustive washing with hexane to remove traces of un-reacted coupling reagent. Synthesis of the longer chain (6-[4-(1H-pyrrol-1-yl] phenoxy) hexyl) ferrocene **(1)** was effected by O-alkylation of the aforementioned pyrrolyl phenol using mild reaction conditions, namely K_2CO_3 in acetonitrile. The reaction was complete in 36 hours, and the product was isolated as a bright yellow solid in 92% yield. The compounds were not water soluble but showed excellent solubility in polar solvents, in particular acetonitrile, and trace levels were soluble in buffer solutions such as $LiClO_4$, phosphate buffer, KCl, Tris and NH_4PF_6.

Electrochemical characterisation of co-polymer films formed from 6-[4-(1H-pyrrol-1-yl] phenoxy) hexyl) ferrocene (2)

Compound **(1)** and **(2)** underwent one reversible redox process at E^o = 0.035 V and 0.365 with ΔE of 101 and 92mV respectively vs. Ag/Ag^+ (in acetonitrile containing 0.1M $TBAPF_6$) (Figure 1(a) and (b)). The anodic limit was varied but it was not possible to grow a conductive electroactive film, nor could a clear current signal be obtained for the pyrrole group in the case of **(2).** Homopolymerisation of monomers bearing bulky groups close to the heteroaromatic ring fails in general (Schuhmann 1997) as was found in the case of both compounds **(1)** and **(2),** therefore co-polymerisation using pyrrole was carried out. The co-polymerisation approach enables species with just one pyrrole group to be used, uses lower polymerisation potentials and it is also possible to vary the metal complex content of the resulting co-polymer film (Ochmanska 1989).

Electropolymerisation of pyrrole can be achieved using potential sweeping leading to electrodeposition of a stable adherent polymer film, obtained in an oxidised state which is electrically conducting. The oxidised state contains approximately one positive charge for every 3-4 pyrrole rings (Deronzier 1996). Novel ferrocene derivatives, ((4-(1H-pyrrol-1-yl)phenoxy)carbonyl) ferrocene (**2**) and (6-(4-(1H-pyrrol-1-yl)phenoxy)hexyl) ferrocene **(1)** were co-polymerised with pyrrole in acetonitrile containing 0.1 M tetrabutylammonium hexafluorophosphate ($TBAPF_6$) by anodic oxidation, to produce electroactive conducting polymer films on glassy carbon electrodes. Following electropolymerisation, the films were washed to remove any unbound monomer and characterised using cyclic voltammetry.

In order to optimise the ratio of the ferrocene derivative:pyrrole in the growth solution, experiments were conducted over a range of concentration of ferrocene derivative (1-5 mM), while the concentration of pyrrole varied from 0.1-5 mM. The effect of the number of cycles (1 to 5 cycles) during co-polymerisation was also examined, in order to determine the effect of thickness on electrochemical behavior of the films. Following polymer growth, the polymers were stabilised in fresh electrolyte (0.1 M $TBAPF_6$/ACN) by repeated cycles at a scan rate of 25 mV s^{-1} for 25 cycles. A subsequent scan rate study was performed on each film over the range 1 to 1000 mV s^{-1}. The resulting polymers showed excellent stability in 0.1 M $TBAPF_6$/ACN and i_p vs. scan rate, υ, was linear up to 200 mV s^{-1} with semi-infinite diffusion limiting the current at higher scan rates (i_p linear with respect to $\nu^{1/2}$).

Figure 2(a) displays the cyclic voltammogram for polymer growth of (6-(4-(1H-pyrrol-1-yl)phenoxy)hexyl) ferrocene **(1)** (5 mM) and pyrrole (5 mM) in 0.1 M $TBAPF_6$-ACN over 5 cycles with the Fe $^{2+/3+}$ redox process evident at $E_{1/2}$ = 0.05V vs. Ag/Ag^+, followed by a rise in current over the range 0.6-1V vs. Ag/Ag^+ indicating the oxidation of **(1)** prior to the pyrrole monomer. The cyclic voltamograms obtained showed the expected increase in current with increasing number of cycles consistent with the growth of an electroactive polymer. The electrochemically induced formation of conducting polymer films on an electrode surface involves diffusional transport of the monomer to the surface, its oxidation at an appropriate electrode potential to a radical cation, radical-radical coupling, electrochemical oxidation of the oligomers formed, chain propagation and finally precipitation of the polycationic polymer (Schuhmann 1997). When the

cathodic potential sweep reached +0.8V, the cathodic current was greater than the anodic indicating that a chemical reaction had occurred i.e. nucleation of polymeric structures onto the surface of the electrode.

Films were also formed at 1 and 2 cycles and Figure 2(b) shows the cyclic voltammogram of a 1 cycle polymer film, following growth, cycled in a fresh solution of 0.1 M $TBAPF_6$/ACN over the range -0.2 V to 0.4 V at a 25 mV s^{-1} (25 cycles). Overlaid on the same figure is a polypyrrole film formed (in the absence of **(1)**) under identical conditions with evidence of the conducting polymer background signal. E^o for the immobilised species $Fe^{II/III}$ was 87mV vs. Ag/Ag^+ resulting in a 122 mV positive shift in the formal potential relative to the solution electrochemistry for **(1),** possibly due to an electrostatic influence of the positively charged polypyrrole chain (Ochmanska 1989).

Almost symmetrical oxidation and reduction waves for the polymer integrated Fe centers were obtained, indicative of the surface bound species. The peak current for an ideally responding surface confined reactant is given by equation (1)

$$I_p = \frac{n^2 F^2}{4RT} \nu A\Gamma \qquad (1)$$

Where n is the number of electrons transferred, F is Faradays constant, ν is the scan rate, R is the gas constant, T is the absolute temperature, A is the area of the electrode and Γ is the surface coverage or concentration of the redox active adsorbate in mol cm^{-2} (Rusling 2003). Figure 2(c) shows the effect of scan rate on the redox system of a co-polymer film of **(1)** formed from 5mM **(1)** and 5 mM pyrrole over the range 1- 1000 mV s^{-1}. Well-defined oxidation and reduction waves were exhibited at low scan rates with linear

increases in both anodic and cathodic currents current observed (1 - 200 mV s^{-1}) indicating surface confined behavior. Plots of peak currents vs. scan rate are shown in Figure 3(a) and similar anodic and cathodic slopes indicate that insertion and ejection of anions (PF_6^-) during oxidation and reduction occurred at the same speed. At higher scan rates, 50 - 200 mV s^{-1}, an increase in ΔE_p was observed, indicating that the process of insertion and expulsion of anions in and out of the polymer films was rate limiting at this time scale. These plots were produced from different ratios of (**1**):pyrrole [(1 – 5) : 5] using 1 cycle of co-polymerisation.

At higher scan rates the layer was no longer exhaustively oxidised, the rate of charge transport through the layer influences the voltammetric response and semi-infinite linear diffusion controls the peak current (Rusling 2003) (peak current now increases with $\nu^{1/2}$). The effective diffusion coefficient D_{CT} corresponding to 'diffusion' of either electrons or charge compensating counterions, can be estimated from the well known Randles Sevcik equation (2).

$$i = (2.69 \times 10^5) n^{3/2} A D_{CT}^{1/2} C \nu^{1/2} \qquad (2)$$

Where C is the concentration of electroactive sites within the film. Slow scan rates establish a finite diffusion regime i.e. changes in potential occur at such a time scale that the whole layer experiences the effect, whereas in the non-ideal case, films are thick (finite diffusion does not occur over the whole film) or there is slow heterogeneous kinetics. Many such systems exhibit behavior that is intermediate between 2 limiting

cases finite and semi-infinite (rate limiting charge transfer through film) (Rusling 2003). The slope of the linear portion of the i_p vs. $\nu^{1/2}$ plots (data not shown) for films formed from 1 cycle growth (1-5 mM ferrocene derivative **(1)** and 5 mM pyrrole) enabled estimation of the product $D_{CT}^{½} C$ (as film thickness was unknown it was not possible to calculate the concentration of sites within the film (C)). The cathodic $D_{CT}^{½} C$ > anodic $D_{CT}^{½} C$ in all cases indicating that anion (PF_6^-) ejection was facile relative to anion insertion into the film for charge compensation during redox switching of the $Fe^{II/III}$ couple. Values for $D_{CT}^{½} C$ decreased from $2.3x10^{-9}$ cm^{-1} s^{-1} mol (5:5) to $1.52x10^{-9}$ cm^{-1} s^{-1} mol (2.5:5) to $1.05x10^{-9}$ cm^{-1} s^{-1} mol (1:5) as expected reflecting the decreased redox active concentration (C) within the film.

Table 1 presents the average electrochemical data set from multiple scan cyclic voltammetric studies on three sets of polymer films formed from different ratio of Fc **(1)** and pyrrole, co-polymerised at 100 mV s^{-1} using 1 cycle. The surface coverage (Γ) can be determined by measuring the Faradaic charge (Q) passed during exhaustive electrolysis e.g. using slow scan rate voltammetry, and values were observed to increase with the ratio of Fc derivative (**1**) used in the growth solution, as expected (from 0.88-$1.81x10^{-8}$ mol cm^{-2}). The stability of the films upon cycling (following growth) was expressed as % decrease in electroactivity for both anodic and cathodic peaks $i_{p(a)}$ and $i_{p(c)}$. The low <10% values obtained in the case of all films examined, was indicative of the stable and adherent nature of the films formed under these conditions.

For an ideal Nernstian reaction under Langmuir isotherm conditions, $E_{pa} = E_{pc}$ or $\Delta E = 0$ (Rusling 2003). Due to the polymeric nature of the films, such ideal behavior was not observed and ΔE values increased with increasing scan rate. It was also observed that the ΔE values increased with increasing concentration of ferrocene derivative **(1)**. Overall, this may reflect a limitation due to anion movement into and out of the polymer during redox switching, together with decrease of charge transport properties in the films. This was less evident in the thinner film formed from 1 mM **(1)** indicating relatively rapid electron transfer.

At low scan rates films exhibited a linear (r^2=0.985) dependence of log (peak current) vs. log (scan rate) for both oxidation and reduction currents (data not shown), with slopes in the range 0.81-0.84 for films formed 1-5 mM **(1)** with 5 mM pyrrole. Co-polymer films formed from 1mM **(1)** and 0.1-1 mM pyrrole resulted in slope values close to 1 (0.91-0.97) for all films. Both sets of data indicated Nernstian equilibrium (Ochmanska 1989) while a decreased in slope to 0.5 would indicate that the Fe electrochemistry is diffusion limited or may be due to ionic resistance of the film i.e. the peak current is limited by the rate of counter-ion migration into or out of the film. The relatively lower values for the thicker films formed from 1-5mM **(1)** suggests some degree of kinetic limitation.

For an ideal Nernstian reaction where the redox centers do not interact laterally a surface confined species will follow the relationships $E_{pa} = E_{pc}$ and (Rusling 2003).

$$FWHM = 3.53\frac{RT}{nF} = \frac{90.6}{n}mV \qquad (3)$$

The full width at half peak maximum (FWHM) values of the films (data shown in Table 1) obtained were higher than the ideal value in particular in the case of the films formed from 2.5 and 5 mM **(1).** No significant difference was observed in the $FWHM_{ox}$ and $FWHM_{red}$ values of the films formed from 2.5:5 and 5:5 mM films. This indicated that oxidation and reduction of the polymer films was almost equally facile.

According to Laviron 1979, for a surface-confined electroactive species with a small enough concentration, the charge transfer coefficient (α) and the charge transfer rate constant (k_s) for electron transfer between the surface confined layer and the electrode can be obtained. A plot of $E_P = f(\log \nu)$ (Figure 4) yields the typical curves with two straight lines with slopes equal to -2.3RT/ αnF and 2.3RT/(1- α)nF for cathodic and anodic peaks, respectively. Transfer coefficient (α) values of 0.5, 0.59 and 0.52 were obtained for films formed using **(1):**pyrrole ratios 5:5, 2.5:5 and 1:5 respectively with k_s values of 0.11, 0.21 and 0.58 s^{-1}.

The effect of the concentration of pyrrole on the co-polymerisation of (6-(4-(1H-pyrrol-1-yl)phenoxy)hexyl)ferrocene was also examined. As no film formation too place at concentrations of pyrrole <0.1 mM, this study examined films formed using pyrrole concentration over the range 0.1 -1 mM. Table 2 presents the average results from cyclic voltammetric studies on three sets of co-polymer films formed from different ratios of **(1)** and pyrrole, co-polymerised at 0.1 mV s^{-1} over 2 cycles and Figure 3(b) shows the i_p vs. ν plots which were linear up to 200mV s^{-1}. Surface coverage values for these films were lower relative to those in Table 1, ranged from 2.2 -8.5x10^{-9} mol cm^{-2} and increased with

increasing pyrrole concentration, indicating the incorporation of more of the redox species **(1).**

With respect to film stability the $i_{p(a)}$ and $i_{p(c)}$ loss (%) for the co-polymer films of ratio 1 : 0.5 were between 1.3-6.3%, and were relatively more stable than the thicker films shown in Table 1. FWHM values were close to ideal for the 1:0.1 mM film as were ΔE_p values and there was less dependence of both ΔE_p and $E_{1/2}$ on scan rate in particular in the case of the thinner films, indicating more ideal reversible behavior and faster electron transfer. Laviron data analysis (plot not shown) resulted in charge transfer co-efficient of 0.72 for the cathodic process with $k_s = 0.57\ s^{-1}$. The linear region of i_p vs $v^{½}$ enabled $D_{CT}^{½} C$ vales to be obtained with cathodic $D_{CT}^{½} C$ > anodic $D_{CT}^{½} C$ as before. Average values decreased from $1.6x10^{-8}$ to $7.13x10^{-9}$ $cm^{-1}\ s^{-1}$ mol as pyrrole concentrations in the growth solution varied from 0.1-1mM with constant concentration **(1)** (1 mM). This could possibly reflect a decreasing C term (as indicated by the trend in surface coverage shown above) or may reflect more rapid charge transfer for the film formed from 1 mM **(1):**1 mM pyrrole.

Effects of reduction switching potential on the electrical conductivity of (6-(4-(1H-pyrrol-1-yl)phenoxy) hexyl)ferrocene co-polymer films

The electrical conductivity of polypyrrole is known to be a function of its oxidation state and hence of the applied potential. The oxidised polymer is highly conductive and the reduced form is semi-conductive or nearly insulating. Over the range 0 - 0.4 V vs. Ag/ Ag^+, conductivity of polypyrrole is constant. At more negative potentials, conductivity

becomes potential dependent and can drop by up to six orders of magnitude. The stability of the Fe $^{II/III}$ redox couple upon increasingly negative switching (reduction) potential (-1.2-0.2V) was examined (Figure 4) up to the positive limit 0.4 V vs. Ag/Ag^{+}. It was observed that the polymeric backbone signal was regenerated upon switching from insulating to conducting state but the redox Fe $^{II/III}$ couple started to diminish (in particular the cathodic wave) when the negative potential was extended beyond -0.6 V.

Co-polymerisation of (6-(4-(1H-pyrrol-1-yl)phenoxy) hexyl)ferrocene and pyrrole using chronocoulometry

Chronocoulometry is an alternative method to potential cycling for conducting polymer film formation. This technique involves measurement of the charge vs. time response to an applied potential step waveform. The technique is useful for measuring adsorption of electroactive species, and the mechanisms and rate constants for chemical reactions coupled to electron transfer reactions (Bard 2001). The process was commenced at a potential (Initial E = 0 V) at which there was no electrolysis and then changed instantaneously (stepped) to a value that leads to oxidation or reduction of the species in solution (0.65 V in this case) and was held at that potential for a user-defined time period. Films were formed using 1 mM **(1)** and 0.5 mM pyrrole with charges passed of 2.21 x 10^{-6}, 8.13 x 10^{-5} and 1.11 x 10^{-5} C and corresponding Γ values of 3.26 x 10^{-10}, 1.19 x 10^{-9}, and 1.63 x 10^{-9} mol cm^{-2} respectively. Following growth, films were stabilised as before and Figure 5(b) shows films formed using different charges passed during chronocoulometry.

Electrochemical characterisation of co-polymer films formed from ((4-(1H-pyrrol-1-yl)phenoxy)carbonyl)ferrocene (1) and pyrrole

Co-polymerisation of ((4-(1H-pyrrol-1-yl)phenoxy)carbonyl)ferrocene **(2)** and pyrrole was performed using potential cycling. Optimisation of growth conditions was performed as before, by variation of both **(2)** (1-5mM) with constant pyrrole concentration (5mM) and fixed concentration of **(2)** (1 mM) with 0.5-1 mM pyrrole. These studies were carried out using a fixed number of growth cycles (optimum was found to be 2 cycles).

Figure 6 (a) shows the film deposition of ((4-(1H-pyrrol-1-yl)phenoxy)carbonyl) ferrocene (1 mM) and pyrrole (0.5 mM) over 2 cycles with E^o for the Fe (II/III) redox couple at 0.37 V vs. Ag/Ag^+. As before, the pyrrole monomer oxidation wave was evident at 0.9 V vs. Ag/Ag^+ and increased currents upon cycling indicates deposition of the redox species onto the electrode surface. Figure 6(b) shows the cyclic voltammogram of the co-polymer films, following polymer growth, being stabilised in a fresh solution of 0.1M $TBAPF_6$/ACN over the range +0.2 V to 0.7 V at 25 mV s^{-1} for 25 cycles. E^o for the film Fe (II/III) couple was 0.447 V vs. Ag/Ag^+ with a positive shift of 80 mV relative to the solution electrochemistry.

The effect of scan rate on the peak currents for the stabilized film grown from 1mM (**2**) and 0.5 mM pyrrole are shown in Figure 7(a). The study was conducted over the scan rate range of 1- 1000 mV s^{-1} in 0.1 M $TBAPF_6$/ACN. Linear increases in current for both

cathodic and anodic peaks over the range 1 - 200 mV s^{-1}, were observed (first 5 cycles are shown here), following which films exhibited semi-infinite diffusion behaviour.

Table 3 and 4 present the average results from three sets of co-polymer films formed from different ratios of (**2**) and pyrrole, co-polymerised at 100 mV s^{-1} for 2 cycles. With respect to Table 3 data the surface coverage (Γ) values were observed to increase with the ratio of Fc derivative (**2**) (4.9-6.7x10^{-9} mol cm^{-2}) as expected. FWHM values, on average, were similar to films formed from **(1)**. E^o was stable with respect to scan rate over the range 0-200 mV s^{-1} with an increase in ΔE as scan rate increased suggesting a kinetic limitation as before. Films showed excellent stability upon cycling with % decrease in electroactivity <6.7% under these conditions. The linear region of i_p vs $v^{½}$ enabled $D_{CT}^{½}$ C vales to be obtained with cathodic $D_{CT}^{½}$ C > anodic $D_{CT}^{½}$ C as for **(1).** Films grown from 5 mM **(2):** 5 mM pyrrole resulted in an average $D_{CT}^{½}$ C value of 2.4 x10^{-9} cm^{-1} s^{-1} mol, 2.25x10^{-9} cm^{-1} s^{-1} mol (2.5:5 mM) and 3.3 x10^{-9} cm^{-1} s^{-1} mol (1:5) with no trend evident with increasing concentration of **(2)** in the growth solution. Slopes of log I_p vs. log v plots for all films grown under these conditions were in the range 0.88-0.99 (very close to the ideal value of 1 indicating Nernstian equilibrium.

Table 4 summarises the electrochemical data for films grown from constant (1 mM) **(2)** and 1-0.5 mM pyrrole. Surface coverage, FWHM values and stability data were similar to films presented in Table 3, and E^o was stable with respect to scan rate over the range 0-200 mV s^{-1} with increasing ΔE. Laviron analysis (plots not shown) resulted in cathodic transfer coefficients (α_c) of 0.36 and 0.35 with k_s = 1.12 s^{-1} and 1.79 s^{-1} for films grown

from 1:1 and 1: 0.5, **(1):**pyrrole respectively. The linear region of i_p vs. $\nu^{1/2}$ enabled $D_{CT}^{1/2}$ C vales to be obtained and values decreased from 5.25×10^{-10} to 3.68×10^{-10} cm^{-1} s^{-1} mol as pyrrole concentrations in the growth solution varied from 1-0.5 mM with constant concentration **(1)** (1 mM). These values are an order of magnitude lower than those determined using data from films grown at higher concentration of pyrrole monomer.

Effects of reduction switching potential on the electrical conductivity of ((4-(1H-pyrrol-1-yl)phenoxy)carbonyl)ferrocene (1) co-polymer films.

Figure 7(b) shows the stability of the redox couple upon increasingly negative switching (reduction) potential (-1.2-0.2V) up to the positive limit 0.7 V vs. Ag/Ag^+. The redox signal for $Fe^{II/III}$ decreased upon cycling with increasingly negative cathodic switching potential, but retention of the background signal and the typical polypyrrole features (-0.3-0V vs. Ag/Ag^+) was achieved, indicating regeneration and stability of the electroactive conducting polymer film.

Chronocoulometry was also employed for ((4-(1H-pyrrol-1-yl)phenoxy) carbonyl) errocene/pyrrole film formation, however a very weak redox couple was evident in the case of this compound (similar conditions to growth of films from **(1)** were employed) and films were not suitable for further evaluation.

Electrochemical stability of ferrocene co-polymer films in aqueous medium

The co-polymer films were also assessed for their electrochemical behavior in a range of aqueous medium such as 0.1 M PBS pH 7.4; 0.1 M KCl in 0.1 M PBS pH 7.4; 0.1 M

NH_4PF_6- aqu; 0.1 M $LiClO_4$- aqu and 0.1 M Tris pH 7.4. Following polymer growth from acetonitrile containing $TBAPF_6$ or $LiClO_4$ both co-polymer films displayed poor redox behavior in aqueous medium indicating limited application in aqueous sensing applications as electrocatalyts or redox mediators. A redox couple at E^o = 0.4 V vs. Ag/AgCl was observed for a copolymer film based on **(2)** examined in Tris buffer pH 6.5 but poor stability prevented any further investigation. Solubility testing of the ferrocene derivatives (**1**) and (**2**) was carried out and (**2**) was slightly more soluble than (**1**) as the latter has a long alkyl chain which rendered the ferrocene derivative more hydrophobic. Hence polymer growth on (**2**) was performed in a range of mixtures of acetonitrile and aqueous medium containing $LiClO_4$. Unfortunately, it was observed that the moderate solubility of (**2**) in mixtures of acetonitrile and aqueous containing $LiClO_4$ was not adequate for co-polymerisation to occur.

Conclusion

The successful synthesis and characterisation of new ferrocene derivatives and (6-(4-(1H-pyrrol-1-yl)phenoxy)hexyl) ferrocene (**1**) and ((4-(1H-pyrrol-1-yl)phenoxy)carbonyl) ferrocene (**2**) was achieved followed by their immobilisation as redox active films by co-electrodeposition with pyrrole. To our knowledge this is the first such report based on these short and long chain ferrocene derivatives with optimisation of growth conditions and thin film evaluation. Film growth using potential sweeping was found to be most suitable for adherent film formation with well defined redox electrochemistry and surface confined behavior.

These functionalised polypyrrole materials were easy to deposit from non-aqueous electrolytes and have potential applications in electronic or sensor devices. Understanding key factors that control electron transfer and charge transport through such polymeric films is an important step in their evaluation as functioning sensor elements. Such hybrid materials combine the electronic conductivity of conducting polymers with the redox properties of metal complexes with the potential to mediate electron transfer reactions. A key feature is metal co-ordination directly to the conjugated polymer backbone, facilitating electronic interaction between the electroactive metal centers and the polymer backbone (Pickup 1999). The materials described here have potential electrocatalytic applications in non-aqueous environments, such as determination of poorly water soluble pollutants. Additional development could employ mixed metal complex co-deposition for electrocatalytic applications requiring multiple electronic steps. Further work in our group is focused on the synthesis and deposition of new hydrophilic ferrocene pyrrole/thiophene derivatives. The extension of the methodology will include electro-entrapment of oxidase enzymes into well characterised polymer matrices bearing redox functionalities, and subsequent evaluation of their mediating properties.

References.

Bard A.J. and L. R. Faulkner. 2001. Electrochemical Methods, Fundamentals and Applications, Second edition, John Wiley & Sons.

Bartlett, P. N. and P.Tebbutt, R. G Whitaker. 1991. Kinetic aspects of the use of modified electrodes and mediators in bioelectrochemistry. Progress in Reaction Kinetics and Mechanisms, 16: 55-155.

Brown, K. L, and J. S Pinter, K. L. Ewing, T. R., Ruch, M. Ambrose, I. Hesslesweet., 2005. Amperometric Detection of Glucose Involving Electropolymerized Tetraaminophthalocyanine and Ferrocene Films. Analytical Letters 38:769-780.

Cass, A. E. G. and G. Davis, G. D. Francis, H. Hill, W. J. Aston, I. J. Higgins, E. V Plotkin, L. D. L Scott, A. P. F.Turner, 1984. Ferrocene-Mediated Enzyme Electrode For Amperometric Determination Of Glucose. Analytical Chemistry. 56:4: 667-671.

Chen, J. and C. O. Too, G. G. Wallace, G. F. Swiegers, B. W. Skelton, A. H. White. 2002. Redox-active conducting polymers incorporating ferrocenes. Preparation, characterization and bio-sensing properties of ferrocenylpropyl and -butyl polypyrroles. Electrochimica Acta. 47 26: 4227-4238.

Deronzier, A. and J-C. Moutet. 1996. Polypyrrole films containing metal complexes; synthesis and application. Co-ordination Chemical Reviews. 147:339-371.

Forrow, N. J. and, Bayliff, S. W. 2005. A commercial whole blood glucose biosensor with a low sensitivity to hematocrit based on an impregnated porous carbon electrode. Biosensors & Bioelectronics. 21 4:581-587.

Forrow, N. J. and G. S., Sanghera, and S. J. Walters. 2002. The influence of structure in the reaction of electrochemically generated ferrocenium derivatives with reduced glucose oxidase. J. Chem. Soc., Dalton Trans. 3187-3194.

Habermuller, K. and A. Ramanavicius, V. Laurinavicius,W. Schuhmann. 2000. An Oxygen-Insensitive Reagentless Glucose Biosensor Based on Osmium-Complex Modified Polypyrrole. Electroanalysis. 12:1383-1389.

Hudson, R. D. A. Ferrocene polymers: current architectures, syntheses and utility. 2001. Journal of Organometallic Chemistry. 637: 47-69.

Koide, S. and K. Yokoyama. 1991. Electrochemical characterization of an enzyme electrode based on a ferrocene-containing redox polymer. Journal of Electroanalytical Chemistry. 468: 193-201.

Laviron E. 1979. General expression of the linear potential sweep voltammogram in the case of diffusionless electrochemical systems. Journal of Electroanalytical Chemistry 101:19-28.

Lasalle, A. L. and B. Limoges, C. Degrand. 1994. Determination of alkaline phosphatase using a Nafion-modified electrode. Journal of Electroanalytical Chemistry 379 1-2: 281-291.

Naruhide, S. and Hirokazu, O. 2008. Development of single-wall carbon nanotubes modified screen-printed electrode using a ferrocene-modified cationic surfactant for amperometric glucose biosensor applications. Sensors and Actuators B 129: 188-194.

Ochmanska J. and P.G. Pickup. 1989. Conducting polypyrrole films containing [Ru (2, 2'-bipyridine) 2(3-{pyrrol-1-ylmethyl} pyridine) Cl] $^{+}$ Electrochemistry, spectroelectrochemistry, electronic conductivity and ionic conductivity. J. Electroanalytical Chemistry. 272:83-105.

Pickup P.G. 1999. Conjugated metallopolymers. Redox polymers with interacting metal based redox sites. J. Mater Chem. 9:1641-1653.

Rahman, M. A. and P. Kumar. D. S Park. 2008. Electrochemical Sensors Based on Organic Conjugated Polymers**.** Sensors. 8, 1: 118-141.

Reiter, S. and K. Habermuller, W. Schuhmann. 2001. A reagentless glucose biosensor based on glucose oxidase entrapped into osmium-complex modified polypyrrole films Sensors and Actuators B 79:150- 156.

Ruan, C. and Y. Li. 2001. Detection of zeptomolar concentrations of alkaline phosphatase based on a tyrosinase and horse-radish peroxidase bienzyme biosensor. Talanta 54 6: 1095-1103.

Rusling J.F. and R.J. Forster. 2003. Electrochemical catalysis with redox polymer and poly-ion-protein films. J. of Colloid and Interface Science. 262:1-15.

Ryabov, A. D., V. S. Sukharev, L. Alexandrova, 2001. New synthesis and new bio-application of cyclometalated ruthenium(II) complexes for fast mediated electron transfer with peroxidase and glucose oxidase. Inorganic Chemistry. 40, 25: 6529-6532**.**

Schuhmann W. and C. Kranz, J. Huber, H.Wohlschlager. 1993. Conducting polymer-based amperometric enzyme electrodes. Towards the development of miniaturized reagentless biosensors. Synth. Met. 61: 31-35.

Schuhmann ,W. and C. Kranz, H. Wohlschlager and J. Strohmeier. 1997. Pulse technique for the electrochemical deposition of polymer films on electrode surfaces. Biosensors and Bioelectronics. 12, 12:1157-1167.

Tustin, G. J. and V.G.H. Lafitte, C. E. Banks. 2007. Synthesis and characterisation of water soluble ferrocenes: Molecular tuning of redox potentials. Journal of Organometallic Chemistry. 692, 23: 5173-5182.

Vorotynstev, M.A. and S. V. Vasilyeva. 2008. Metallocene-containing conjugated polymers. Advances in Colloid and Interface Science 139:97-149.

Warren, S. and R. Doaga, T. McCormac, E. Dempsey. 2008. Electrochemical studies of osmium-(pyrrole-methyl) pyridine-co-polymers deposited using the membrane template method. Electrochimica Acta. 53 13: 4550-4556.

Table 1. Average data (n=3) multiple scan cyclic voltammetric study on co-polymer films of (6-(4-(1H-pyrrol-1-yl)phenoxy)hexyl)ferrocene (1-5mM) and pyrrole (5 mM) formed using 1 cycle of co-polymerisation and examined in acetonitrile/0.1 M $TBAPF_6$ following stabilisation for 25 cycles at 25 mV s^{-1}

Ratio of ferrocene : pyrrole (mM)	10^8 Γ (mol/cm^2)	$i_{p(a)}$ loss (%)	$i_{p(c)}$ loss (%)	Scan rate (mV s^{-1})	ΔE (mV)	E^o (mV)	$FWHM_{ox}$ (mV)	$FWHM_{red}$ (mV)
1 : 5	0.88	6.4	5.2	1	25	91	128	130
				5	24	93		
				10	39	92		
				20	58	93		
				50	116	92		
				100	186	98		
				200	182	126		
2.5 : 5	1.40	2.5	2.2	1	17	87	140	138
				5	33	85		
				10	53	85		
				20	84	85		
				50	160	85		
				100	254	87		
				200	307	90		
5 : 5	1.81	4.4	4.2	1	18	103	188	140
				5	34	101		
				10	49	102		
				20	82	102		
				50	151	102		
				100	244	105		
				200	327	132		

Table 2. Average data (n=3) multiple scan cyclic voltammetric study on co-polymer films of (6-(4-(1H-pyrrol-1-yl)phenoxy)hexyl)ferrocene (1mM) and pyrrole (0.1-1 mM) formed from 2 cycles of co-polymerisation and examined in acetonitrile/0.1 M $TBAPF_6$ following stabilisation for 25 cycles at 25 mV s^{-1}

Ratio of ferrocene : pyrrole (mM)	10^8 Γ (mol/cm^2)	$i_{p(a)}$ loss (%)	$i_{p(c)}$ loss (%)	Scan rate (mV s^{-1})	ΔE_p (mV)	E^o (mV)	$FWHM_{ox}$ (mV)	$FWHM_{red}$ (mV)
1 : 0.1	0.220	1.3	3.6	1	13	81	112	108
				5	15	80		
				10	13	80		
				20	18	79		
				50	27	81		
				100	41	82		
				200	71	83		
1 : 0.25	0.317	6.5	6.3	1	11	77	114	110
				5	15	79		
				10	18	79		
				20	21	79		
				50	36	80		
				100	53	81		
				200	88	82		
1 : 0.5	0.594	5.7	3.6	1	16	84	182	172
				5	15	78		
				10	21	77		
				20	30	80		
				50	61	80		
				100	101	81		
				200	172	78		
1 : 1	0.856	1.9	2.5	1	15	76	132	148
				5	17	77		
				10	25	78		
				20	37	79		
				50	78	79		
				100	126	81		
				200	207	81		

Table 3. Average data (n=3) multiple scan cyclic voltammetric study on co-polymer films of ((4-(1H-pyrrol-1-yl)phenoxy)carbonyl) ferrocene (1-5mM) and pyrrole (5 mM) dpyrrole (in acetonitrile containing 0.1 M $TBAPF_6$ formed from 2 cycles of co-polymerisation and examined in acetonitrile/0.1 M $TBAPF_6$ following stabilisation for 25 cycles at 25 mV s^{-1}

Ratio of ferrocene : pyrrole (mM)	10^9 Γ (mol/cm^2)	$i_{p(a)}$ loss (%)	$i_{p(c)}$ loss (%)	Scan rate (mV s^{-1})	ΔE_p (mV)	E^o(V)	$FWHM_{ox}$ (mV)	$FWHM_{red}$ (mV)
1 : 5	4.9	1.0	5.6	1	27	0.46	149	140
				5	23	0.48		
				10	36	0.48		
				20	75	0.48		
				50	98	0.48		
				100	121	0.49		
				200	198	0.49		
2.5 : 5	5.35	1.8	3.4	1	25	0.46	144	138
				5	24	0.48		
				10	37	0.48		
				20	61	0.48		
				50	94	0.48		
				100	99	0.47		
				200	206	0.48		
5 : 5	6.67	5.9	6.2	1	23	0.47	136	136
				5	24	0.48		
				10	33	0.48		
				20	36	0.48		
				50	61	0.48		
				100	101	0.48		
				200	166	0.48		

Table 4. Average data (n=3) multiple scan cyclic voltammetric study on co-polymer films of ((4-(1H-pyrrol-1-yl)phenoxy)carbonyl) ferrocene (1 mM) with pyrrole (0.5-1 mM) in acetonitrile containing 0.1 M $TBAPF_6$ made from 2 cycles of co-polymerisation, following stabilisation for 25 cycles at 25 mV s^{-1}

Ratio of ferrocene : pyrrole (mM)	$10^9\Gamma$ (mol/cm^2)	$i_{p(a)}$ loss (%)	$i_{p(c)}$ loss (%)	Scan rate (mV s^{-1})	ΔE_p (mV)	E^o (mV)	$FWHM_{ox}$ (mV)	$FWHM_{red}$ (mV)
1 : 0.5	4.5	6.8	6.1	1	28	443	136	140
				5	11	438		
				10	18	438		
				20	20	439		
				50	48	434		
				100	79	440		
				200	126	439		
1 : 1	6.4	5.7	4.2	1	28	404	132	130
				5	26	405		
				10	20	409		
				20	26	402		
				50	31	392		
				100	49	368		
				200	73	332		

Legends for Figures

Scheme 1 Synthesis of (6-[4-(1H-pyrrol-1-yl]phenoxy)hexyl)ferrocene **(1)**

Scheme 2 Synthesis of ([4-(1H-pyrrol-1-yl)phenoxy]carbonyl)ferrocene **(2)**

Figure 1(a) Cyclic voltammogram of (6-(4-(1H-pyrrol-1-yl)phenoxy) hexyl) ferrocene (1 mM) in 0.1M $TBAPF_6$-ACN at a glassy carbon working electrode at 10 mV s^{-1} vs. Ag / Ag^+ $AgNO_3$ (10 mM)

Figure 1 (b) Cyclic voltammogram of ((4-(1H-pyrrol-1-yl)phenoxy) carbonyl) ferrocene (1 mM) in 0.1M $TBAPF_6$-ACN at a glassy carbon working electrode at 10 mV s^{-1} vs. Ag / Ag^+ | $AgNO_3$ (10 mM)

Figure 2(a) Co-polymerisation of (6-(4-(1H-pyrrol-1-yl)phenoxy)hexyl)ferrocene (5 mM) + pyrrole (5 mM) in 0.1M $TBAPF_6$-ACN at 100 mV s^{-1} over 5 cycles

Figure 2(b) Stability of the 6-(4-(1H-pyrrol-1-yl)phenoxy)hexyl)ferrocene co-polymer formed from 1 cycle in 5 mM **(1)** and 5 mM pyrrole in 0.1M $TBAPF_6$-ACN at 25 mV s^{-1} over 25 cycles. Overlaid is background current from a polypyrrole film formed under the same conditions in the absence of **(1)**

Figure 2 (c) Scan rate study with of for co-polymer formed from 5mM **(1)** and 5 mM pyrrole in 0.1M $TBAPF_6$-ACN (1 cycle film – ratio 5:5 mM). Shown are the first 5 cycles.

Figure 3(a) i_p (μA) vs scan rate (mV s^{-1}) for the co-polymer films (6-(4-(1H-pyrrol-1-yl)phenoxy)hexyl)ferrocene in acetonitrile containing 0.1 M $TBAPF_6$ from 1 cycle of co-polymerisation following stabilisation at 25 mV s^{-1} vs. Ag/Ag^+ (25 cycles) I and I' = i_{pa} and i_{pc} for Fc : pyrrole 1 : 5; II and II' = Fc : pyrrole 2.5 : 5; III and III' Fc : pyrrole 5 : 5mM.

Figure 3(b) I_p (μA) vs. scan rate (mV s^{-1}) for the co-polymer films of (6-(4-(1H-pyrrol-1-yl)phenoxy)hexyl)ferrocene in acetonitrile containing 0.1 M $TBAPF_6$ from 2 cycles of co-polymerisation following stabilisation at 25 mV s^{-1} vs. Ag/Ag^+ (25 cycles) I and I' = i_{pa} and i_{pc} for ratio of Fc : pyrrole 1 : 1; II and II' = Fc : pyrrole 1 : 0.5; III and III' = Fc : pyrrole 1 : 0.25; IV and IV' = Fc : pyrrole 1 : 0.1

Figure 4(a) Laviron plot of Ep vs. log v for co-polymer films of (6-(4-(1H-pyrrol-1-yl)phenoxy)hexyl)ferrocene formed from 5mM **(1)** and 5 mM pyrrole in 0.1M $TBAPF_6$-ACN (1 cycle film)

Figure 4(b) Laviron plot of Ep vs. log v for co-polymer films of (6-(4-(1H-pyrrol-1-yl)phenoxy)hexyl)ferrocene formed from 2.5 mM **(1)** and 5 mM pyrrole in 0.1M $TBAPF_6$-CAN (1 cycle film)

Figure 4(c) Laviron plot of Ep vs. log v for co-polymer films of (6-(4-(1H-pyrrol-1-yl)phenoxy)hexyl)ferrocene formed from 1.0 mM (7) and 5 mM pyrrole in 0.1M $TBAPF_6$-CAN (1 cycle film)

Figure 5 (a) Effect of cathodic switching potential on redox process for co-polymer film of (6-(4-(1H-pyrrol-1-yl)phenoxy) hexyl)ferrocene (1 mM) and pyrrole (0.5 mM) formed from 2 cycles of co-polymerisation, following stabilisation.

Figure 5 (b) Comparison of the co-polymer films of (6-(4-(1H-pyrrol-1-yl)phenoxy) hexyl)ferrocene (1 mM) + pyrrole (0.5 mM) formed by chronocoulometry in 0.1M $TBAPF_6$-ACN following cycling at 25 mV s^{-1} over 25 cycles.

Figure 6(a) Co-polymerisation of ((4-(1H-pyrrol-1-yl)phenoxy)carbonyl) ferrocene (1 mM) + pyrrole (0.5 mM) in 0.1 M $TBAPF_6$-ACN at 100 mV s^{-1} over 2 cycles

Figure 6(b) Stability of ((4-(1H-pyrrol-1-yl)phenoxy)carbonyl)ferrocene (1 mM) + pyrrole (0.5 mM) in 0.1M $TBAPF_6$-ACN at 25 mV s^{-1} over 25 cycles

Figure 7(a) Scan rate study of (1 – 200 mV s^{-1}) on ((4-(1H-pyrrol-1-yl)phenoxy) carbonyl)ferrocene (1 mM) + pyrrole (0.5 mM) in 0.1M $TBAPF_6$-ACN

Figure 7(b) Effect of cathodic switching potential on redox process for co-polymer film of ((4-(1H-pyrrol-1-yl)phenoxy) carbonyl)ferrocene (1 mM) and pyrrole (0.5 mM) over 2 cycles of co-polymerisation, following stabilisation.

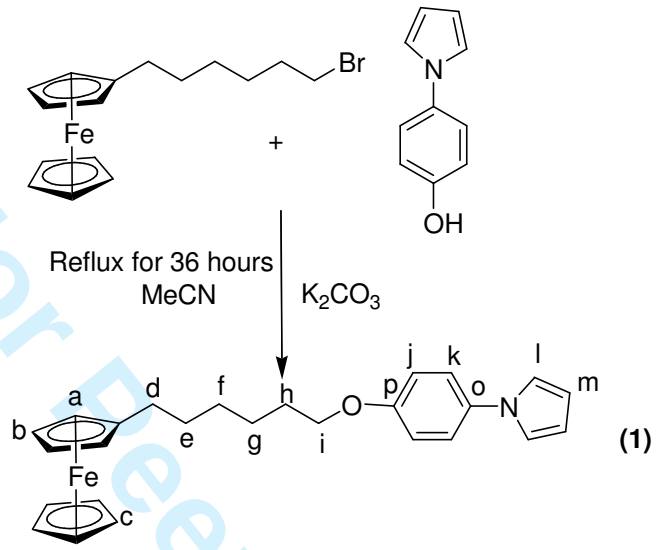

Scheme 1 Synthesis of (6-[4-(1H-pyrrol-1-yl]phenoxy)hexyl)ferrocene **(1)**

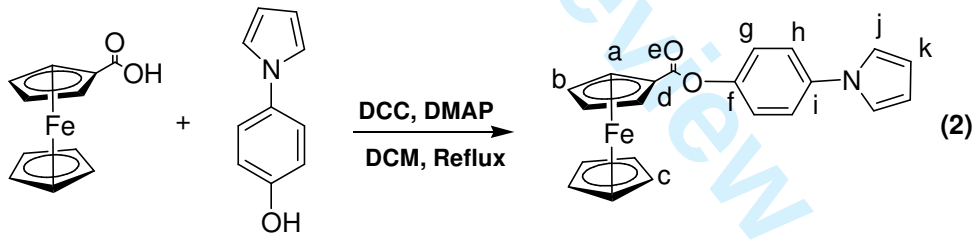

Scheme 2 Synthesis of ([4-(1H-pyrrol-1-yl)phenoxy]carbonyl)ferrocene **(2)**

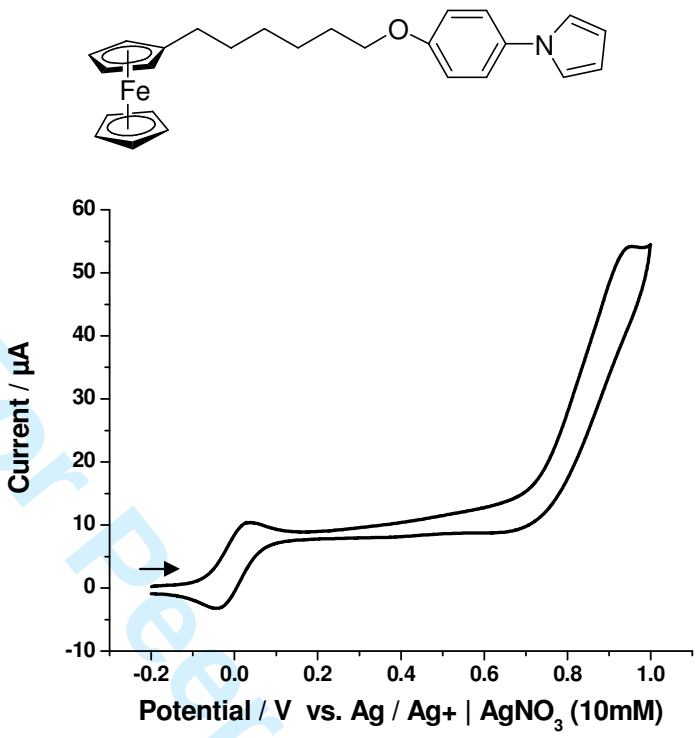

Figure 1(a)
Cyclic voltammogram of (6-(4-(1H-pyrrol-1-yl)phenoxy) hexyl) ferrocene (1 mM) in 0.1M $TBAPF_6$-ACN at a glassy carbon working electrode at 10 mV s^{-1} vs. Ag / Ag^+ $AgNO_3$ (10 mM)

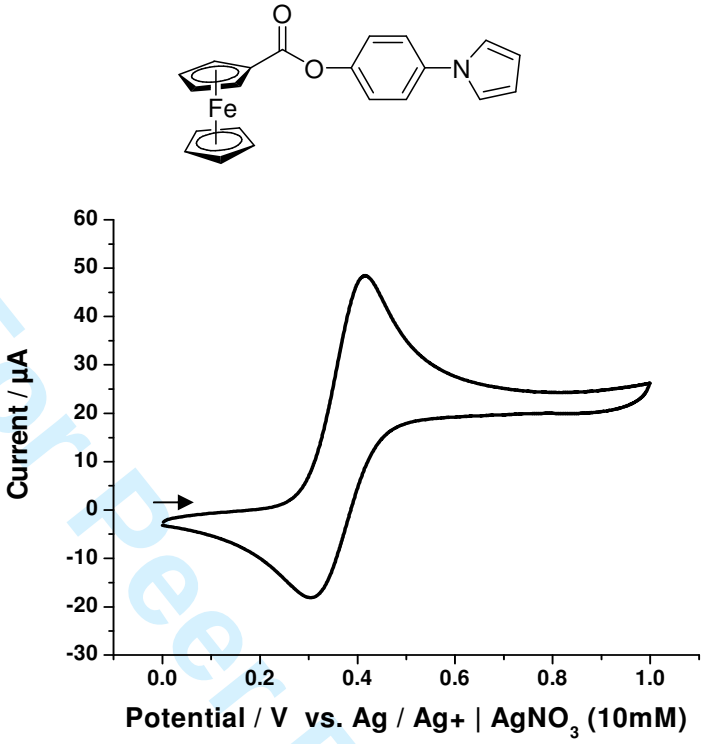

Figure 1 (b)
Cyclic voltammogram of ((4-(1H-pyrrol-1-yl)phenoxy) carbonyl) ferrocene (1 mM) in 0.1M $TBAPF_6$-ACN at a glassy carbon working electrode at 10 mV s^{-1} vs. Ag / Ag^+ | $AgNO_3$ (10 mM)

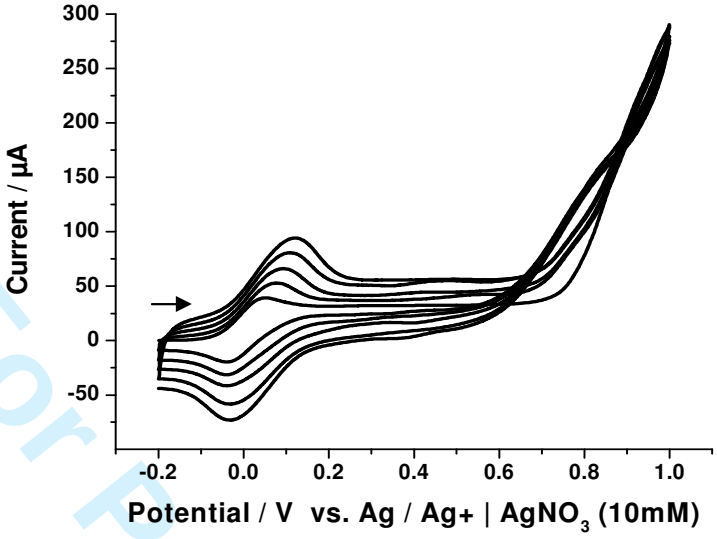

Figure 2(a)
Co-polymerisation of (6-(4-(1H-pyrrol-1-yl)phenoxy)hexyl)ferrocene (5 mM) + pyrrole (5 mM) in 0.1M $TBAPF_6$-ACN at 100 mV s^{-1} over 5 cycles

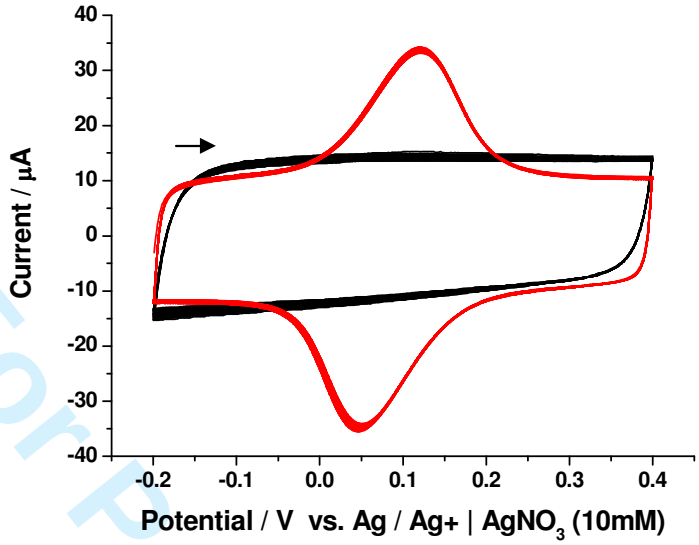

Figure 2(b) Stability of the 6-(4-(1H-pyrrol-1-yl)phenoxy)hexyl)ferrocene co-polymer formed from 1 cycle in 5 mM **(1)** and 5 mM pyrrole in 0.1M $TBAPF_6$-ACN at 25 mV s^{-1} over 25 cycles. Overlaid is background current from a polypyrrole film formed under the same conditions in the absence of **(1)**

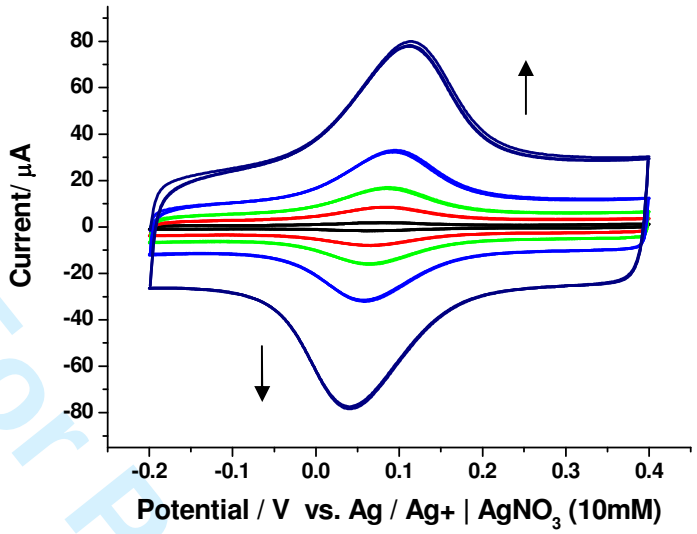

Figure 2 (c)

Scan rate study with of for co-polymer formed from 5mM (7) and 5 mM pyrrole in 0.1M $TBAPF_6$-ACN (1 cycle film – ratio 5:5 mM). Shown are the first 5 cycles.

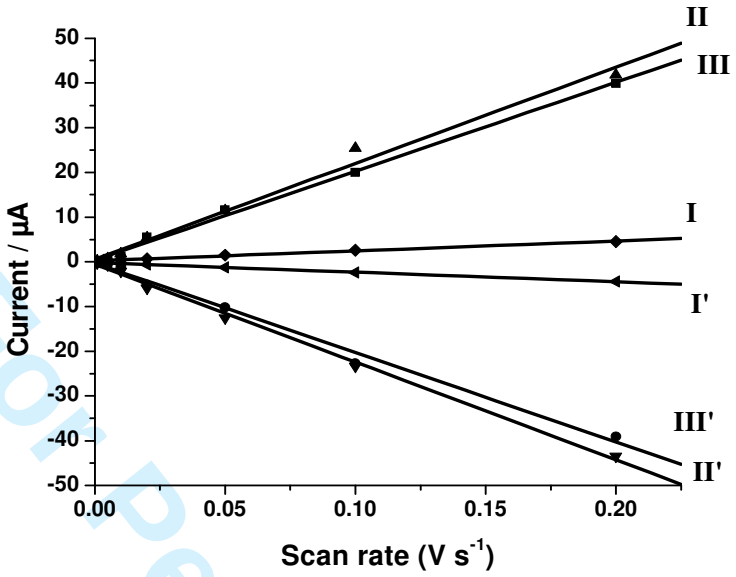

Figure 3(a) i_p (µA) vs scan rate (mV s^{-1}) for the co-polymer films (6-(4-(1H-pyrrol-1-yl)phenoxy)hexyl)ferrocene in acetonitrile containing 0.1 M $TBAPF_6$ from 1 cycle of co-polymerisation following stabilisation at 25 mV s^{-1} vs. Ag/Ag^+ (25 cycles) I and I' = i_{pa} and i_{pc} for Fc : pyrrole 1 : 5; II and II' = Fc : pyrrole 2.5 : 5; III and III' Fc : pyrrole 5 : 5mM.

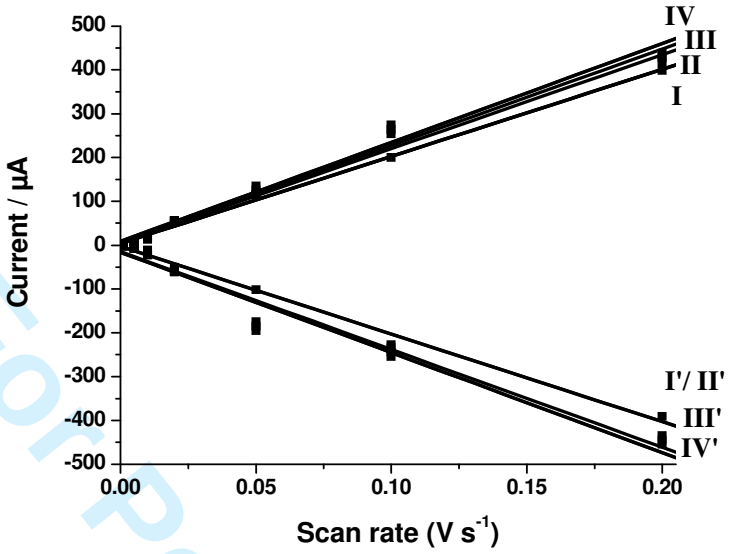

Figure 3(b)

I_p (µA) vs. scan rate (mV s^{-1}) for the co-polymer films of (6-(4-(1H-pyrrol-1-yl)phenoxy)hexyl)ferrocene in acetonitrile containing 0.1 M $TBAPF_6$ from 2 cycles of co-polymerisation following stabilisation at 25 mV s^{-1} vs. Ag/Ag^+ (25 cycles) I and I' = i_{pa} and i_{pc} for ratio of Fc : pyrrole 1 : 1; II and II' = Fc : pyrrole 1 : 0.5; III and III' = Fc : pyrrole 1 : 0.25; IV and IV' = Fc : pyrrole 1 : 0.1

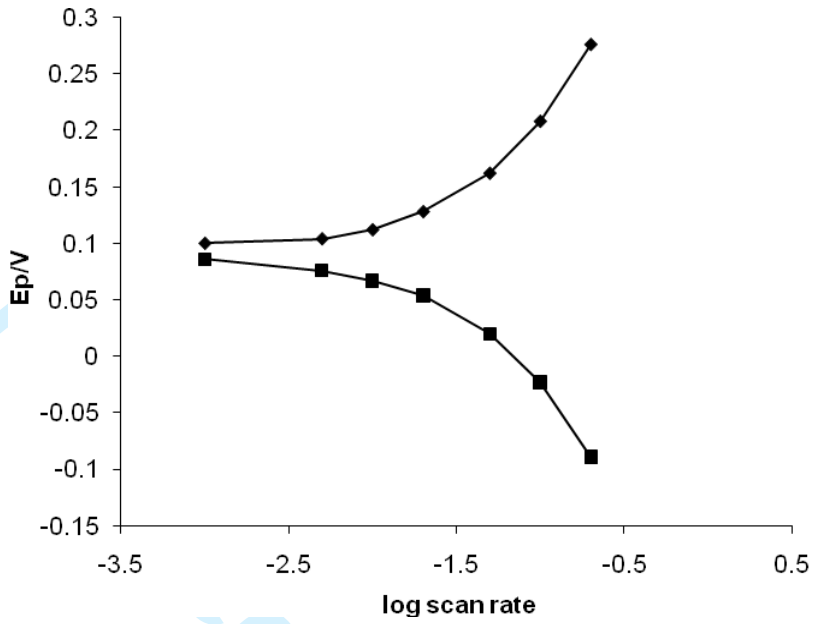

Figure 4(a)
Laviron plot of Ep vs. log v for co-polymer films of (6-(4-(1H-pyrrol-1-yl)phenoxy)hexyl)ferrocene formed from 5mM (7) and 5 mM pyrrole in 0.1M $TBAPF_6$-ACN (1 cycle film)

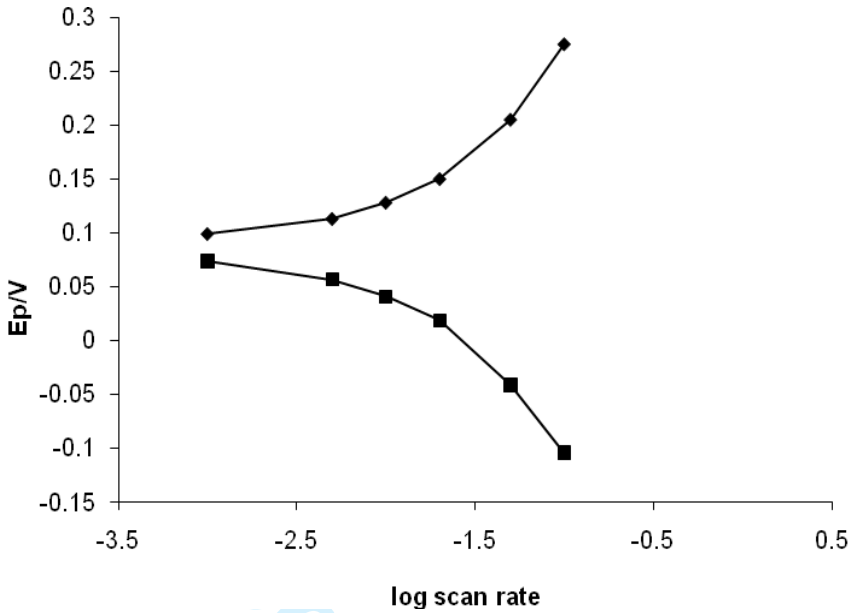

Figure 4(b) Laviron plot of Ep vs. log v for co-polymer films of (6-(4-(1H-pyrrol-1-yl)phenoxy)hexyl)ferrocene formed from 2.5 mM (7) and 5 mM pyrrole in 0.1M $TBAPF_6$-CAN (1 cycle film)

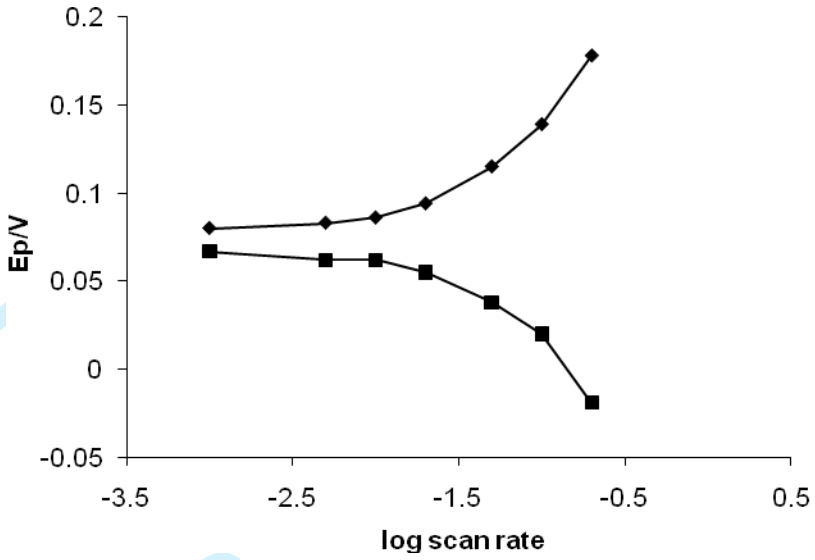

Figure 4(c)
Laviron plot of Ep vs. log v for co-polymer films of (6-(4-(1H-pyrrol-1-yl)phenoxy)hexyl)ferrocene formed from 1.0 mM (7) and 5 mM pyrrole in 0.1M $TBAPF_6$-CAN (1 cycle film)

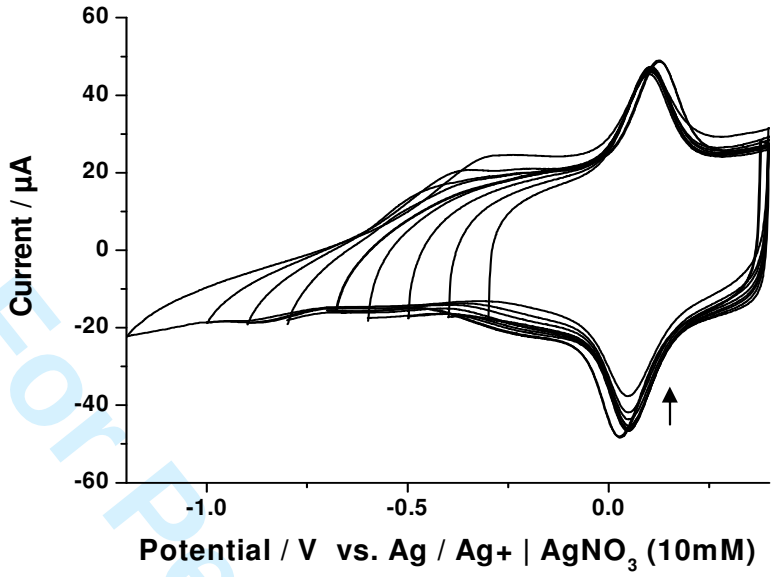

Figure 5 (a)
Effect of cathodic switching potential on redox process for co-polymer film of (6-(4-(1H-pyrrol-1-yl)phenoxy) hexyl)ferrocene (1 mM) and pyrrole (0.5 mM) formed from 2 cycles of co-polymerisation, following stabilisation.

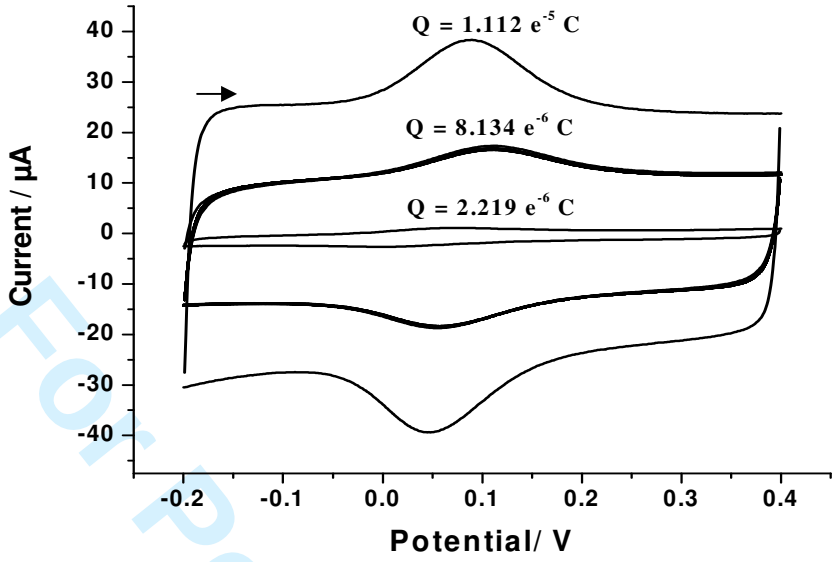

Figure 5 (b)
Comparison of three co-polymer films of (6-(4-(1H-pyrrol-1-yl)phenoxy) hexyl)ferrocene (1 mM) + pyrrole (0.5 mM) formed by chronocoulometry in 0.1M $TBAPF_6$-ACN following cycling at 25 mV s^{-1} over 25 cycles.

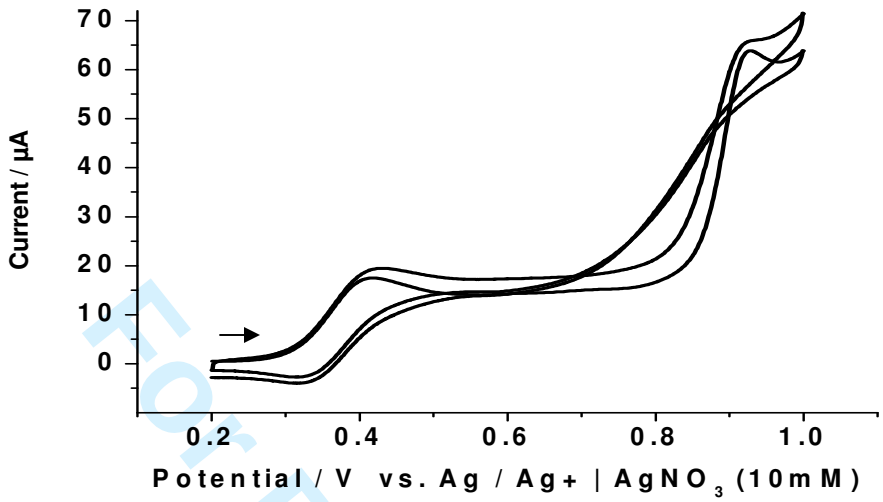

Figure 6(a) Co-polymerisation of ((4-(1H-pyrrol-1-yl)phenoxy)carbonyl) ferrocene (1 mM) + pyrrole (0.5 mM) in 0.1 M $TBAPF_6$-ACN at 100 mV s^{-1} over 2 cycles

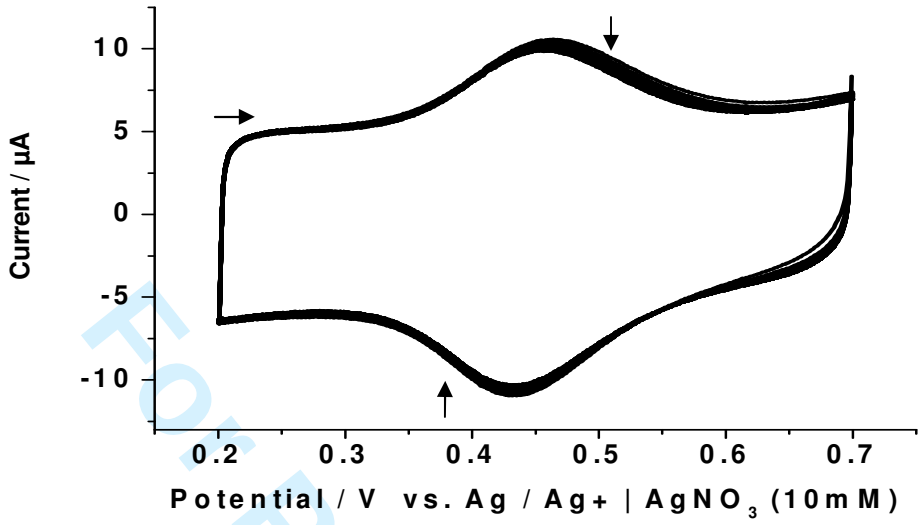

Figure 6(b)
Stability of ((4-(1H-pyrrol-1-yl)phenoxy)carbonyl)ferrocene (1 mM) + pyrrole (0.5 mM) in 0.1M $TBAPF_6$-ACN at 25 mV s^{-1} over 25 cycles

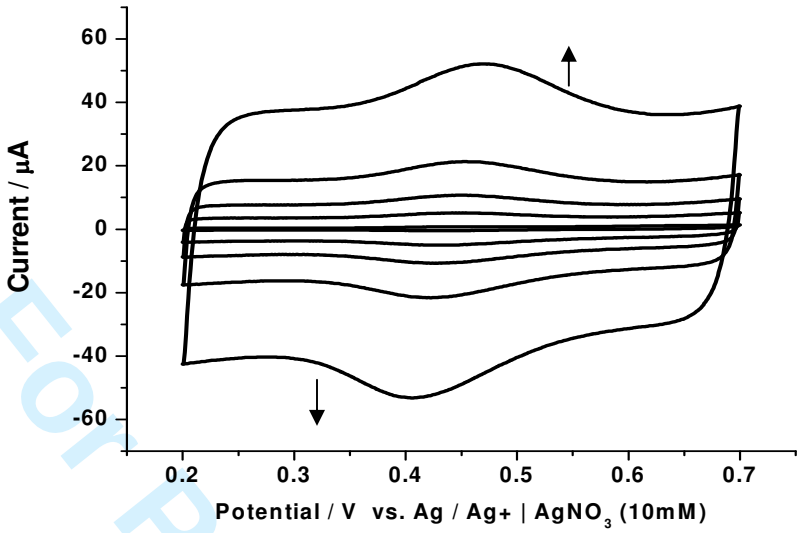

Figure 7(a)
Scan rate study of (1 – 200 mV s^{-1}) on ((4-(1H-pyrrol-1-yl)phenoxy) carbonyl)ferrocene (1 mM) + pyrrole (0.5 mM) in 0.1M $TBAPF_6$-CAN

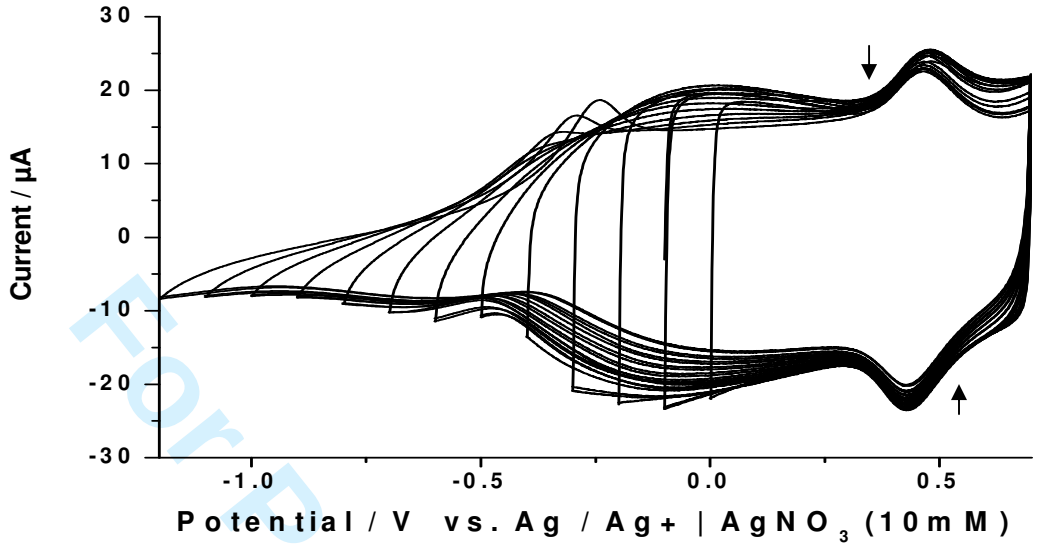

Figure 7(b)
Effect of cathodic switching potential on redox process for co-polymer film of ((4-(1H-pyrrol-1-yl)phenoxy) carbonyl)ferrocene (1 mM) and pyrrole (0.5 mM) over 2 cycles of co-polymerisation, following stabilisation.